

## Transport and tumbling of polymers in viscoelastic shear flow

Sadhana Singh,<sup>1</sup> R. K. Singh,<sup>1,2,\*</sup> and Sanjay Kumar<sup>1</sup>

<sup>1</sup>Department of Physics, Banaras Hindu University, Varanasi 221005, India

<sup>2</sup>Department of Physics, Indian Institute of Technology, Bombay, Powai, Mumbai 400076, India



(Received 29 February 2020; revised 15 June 2020; accepted 19 June 2020; published 10 July 2020; corrected 14 September 2020)

Polymers in shear flow are ubiquitous and we study their motion in a viscoelastic fluid under shear. Employing Hookean dumbbells as representative, we find that the center-of-mass motion follows:  $\langle x_c^2(t) \rangle \sim \dot{\gamma}^2 t^{\alpha+2}$ , generalizing the earlier result:  $\langle x_c^2(t) \rangle \sim \dot{\gamma}^2 t^3$  ( $\alpha = 1$ ). Here  $0 < \alpha < 1$  is the coefficient defining the power-law decay of noise correlations in the viscoelastic media. Motion of the relative coordinate, on the other hand, is quite intriguing in that  $\langle x_r^2(t) \rangle \sim t^\beta$  with  $\beta = 2(1 - \alpha)$ , for small  $\alpha$ . This implies nonexistence of the steady state, making it inappropriate for addressing tumbling dynamics. We remedy this pathology by introducing a nonlinear spring with FENE-LJ interaction and study tumbling dynamics of the dumbbell. We find that the tumbling frequency exhibits a nonmonotonic behavior as a function of shear rate for various degrees of subdiffusion. We also find that this result is robust against variations in the extension of the spring. We briefly discuss the case of polymers.

DOI: [10.1103/PhysRevE.102.012605](https://doi.org/10.1103/PhysRevE.102.012605)

### I. INTRODUCTION

Viscoelastic fluids under shear are ubiquitous, especially in biological systems, and aid in transport of biomolecules *in vivo*. Viscoelasticity, as the name suggests, is the property of a material comprising of both viscous and elastic behavior [1]. Almost all materials with biological or engineering interests are viscoelastic to some degree [2]. The elastic component of the material tends to bring it back to its original configuration when put under stress [3]. As a result, motion in viscoelastic media is generally slower, i.e., the mean-square displacement  $\langle x^2(t) \rangle \sim t^\alpha$  [4], with  $0 < \alpha < 1$ , consequent of the antipersistent correlations in successive displacements [5]. Viscoelastic subdiffusion frequently arises in motion in biological domains, e.g., motion in crowded fluids [6], cytoplasm of living cells [7], locus of a chromosome in eukaryotes [8], etc.

Even though a useful representative of system dynamics, a single-particle description is not fully appropriate when it comes to investigating systems with internal degrees of freedom, e.g., polymers. In addition, polymers constitute the basic building blocks of the macromolecules like DNA and proteins. Hence, it becomes natural to investigate the dynamical aspects of a polymer in viscoelastic media. However, most of the polymer transport *in vivo* takes place in viscoelastic fluids under shear, wherein they not only move but also tumble along, i.e., an end-to-end rotation. The phenomena of polymer tumbling is well understood for the case of viscous shear flows [9,10]. And arises when the relaxation time of the polymer is larger than the timescale of flow deformation [11], with characteristic tumbling time varying sublinearly with the flow rate [12,13]. However, a majority of studies involving tumbling do not cover the practically important case of shear

flows arising in viscoelastic media, e.g., polymer plastics and most of the biological materials [14].

These observations raise an interesting question: What are the dynamical characteristics of a polymer in a viscoelastic fluid under shear? This is a question of immense practical significance, which we answer in the present work employing a dumbbell which is the simplest form of a polymer. For the two masses connected by a harmonic spring, we show both analytically and numerically that the separation grows without bounds. This implies toward the nonexistence of steady state and essentially means that tumbling cannot be addressed using a linear system. We remedy this pathology by introducing a finitely extensible nonlinear elastic spring with repulsive part of the Lennard-Jones interaction (FENE-LJ) [15,16]. Thus, allowing us to address tumbling.

### II. GENERALIZED LANGEVIN EQUATION IN SHEAR FLOWS

The generalized Langevin equation (GLE) [17] describing the motion of a dumbbell in a viscoelastic material under shear reads:

$$\int_0^t dt' \eta(t-t') (\dot{\mathbf{r}}_i - \dot{\gamma} y_i \mathbf{i})(t') = -\nabla_i V(|\mathbf{r}_i - \mathbf{r}_j|) + \xi_i(t), \quad (1)$$

where  $\mathbf{r}_i \equiv (x_i, y_i, z_i)$ , with  $i = 1, 2$  and  $i \neq j$  denote the two particles, and  $\dot{\gamma}$  is the shear rate applied to the viscoelastic fluid. The noise vectors  $\xi_1$  and  $\xi_2$  are Gaussian random variables with correlation matrices:  $\langle \xi_i(t) \xi_j^T(t') \rangle = \delta_{ij} k_B T \eta(|t-t'|) \mathbf{I}_3$ , consistent with the fluctuation dissipation relation [18], where  $\mathbf{I}_3$  denotes the  $3 \times 3$  identity matrix. For the case of harmonically interacting dumbbells we choose  $V(|\mathbf{r}_i - \mathbf{r}_j|) = \frac{1}{2} \omega_0^2 (\mathbf{r}_i - \mathbf{r}_j)^2$ , which is a Rouse polymer of size  $N = 2$  [19].

The term inside the integral in Eq. (1) is the memory kernel representing time-dependent friction. Consequently,

\*rksinghmp@gmail.com

the present state depends on the entire history. Physically, the GLE renders itself derivable in terms of mechanical equations for a particle interacting with a thermal bath, in terms of the spectral density of the bath oscillators [20,21]. To address the problem at hand, we employ a power-law decaying form for the memory kernel:  $\eta(t) = \eta_\alpha t^{-\alpha} / \Gamma(1 - \alpha)$ , with  $0 < \alpha < 1$  [22]. The advantage of this form of memory kernel is that it captures both the viscous and elastic limits for extreme values of the coefficient  $\alpha$ . In other words,  $\lim_{\alpha \searrow 0} \eta(t) = \eta$  (purely elastic) and  $\lim_{\alpha \nearrow 1} \eta(t) = 2\eta\delta(t)$  (purely viscous), where  $\eta$  represents the friction coefficient for either elastic medium or viscous medium [23]. The derivation for the viscous case is provided in Appendix A. With this form of memory kernel, the GLE results in subdiffusive motion at all times [23,24], though it is expected that diffusion emerges at long times in any realistic scenario. More on that later.

### A. Center-of-mass motion for linear spring

Absence of any external force on the dumbbell allows us to separate its dynamics into the motion of center of mass and motion about the center of mass. The coordinate of the center of mass  $(x_c, y_c, z_c) \equiv \mathbf{r}_c = \frac{\mathbf{r}_1 + \mathbf{r}_2}{2}$  evolves as:

$$\int_0^t dt' \eta(t-t') (\dot{x}_c - \dot{y}_c)(t') = \xi_{cx}(t), \quad (2a)$$

$$\int_0^t dt' \eta(t-t') \dot{y}_c(t') = \xi_{cy}(t), \quad (2b)$$

$$\int_0^t dt' \eta(t-t') \dot{z}_c(t') = \xi_{cz}(t), \quad (2c)$$

where  $(x_c, y_c, z_c) = (0, 0, 0)$  at  $t = 0$  and  $\xi_c(t) = [\xi_1(t) + \xi_2(t)]/2$  is Gaussian noise with mean zero and correlation:  $\langle \xi_c(t) \xi_c^T(t') \rangle = \frac{1}{2} k_B T \eta(|t-t'|) \mathbf{I}_3$ . It is evident looking at Eq. (2) that the center of mass moves like a free particle in shear flow. Interestingly, the  $y$  (and  $z$ ) components of motion do not feel the effect of shear flow, with the well-known two-point correlation:  $\langle y(t_1) y(t_2) \rangle = \frac{k_B T}{2\eta_\alpha \Gamma(1+\alpha)} [t_1^\alpha + t_2^\alpha - |t_1 - t_2|^\alpha]$  [4]. The  $x$  component of motion is, however, affected by the presence of shear flow which is directed along the  $x$  axis. Invoking the Laplace transform of Eq. (2) allows us to decouple the convolution of the memory kernel  $\eta$  and local velocity. As a result, the time evolution of the  $x$  coordinate of the center of mass evolves as:

$$x_c(t) = \dot{\gamma} \int_0^t dt' y_c(t') + \int_0^t dt' g(t-t') \xi_{cx}(t'), \quad (3)$$

where  $\tilde{g}(s) = 1/s\tilde{\eta}(s)$ , is the Laplace transform of  $g$ . This allows us to calculate the two point correlation the  $x$  component of motion:

$$\begin{aligned} \langle x_c(t_1) x_c(t_2) \rangle &= \dot{\gamma}^2 \int_0^{t_1} \int_0^{t_2} dt' dt'' \langle y_c(t') y_c(t'') \rangle \\ &+ \int_0^{t_1} \int_0^{t_2} dt' dt'' g(t_1-t') g(t_2-t'') \langle \xi_{cx}(t') \xi_{cx}(t'') \rangle, \end{aligned} \quad (4)$$

where the cross terms vanish due to the independence of the noise components along  $x$  and  $y$  direction. With the integrand

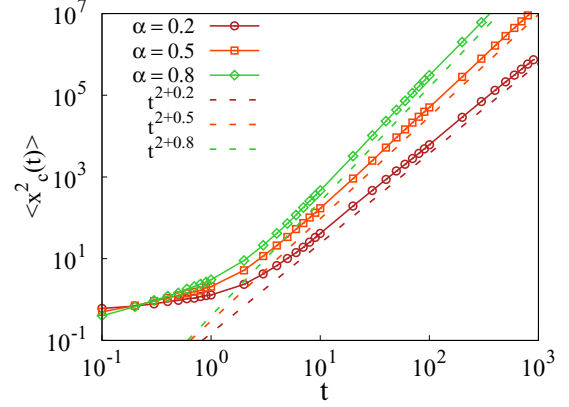


FIG. 1. Mean-square displacement of the center-of-mass motion  $x_c$  along the shear flow direction for varying  $\alpha$ , with respective line fits. Parameter values for numerical calculation are:  $\dot{\gamma} = 1$ ,  $\eta_\alpha = 1$  and  $k_B T/2 = 1$ .

of the first term going as  $t^\alpha$  and  $g(t) \sim t^{\alpha-1}$ , it follows that the two-point correlation increases as a power law in time, with exponent reading  $\alpha + 2$  for the first term and  $\alpha$  for the second term. As a consequence, the mean-square displacement for the center-of-mass motion along the shear flow reads:

$$\langle x_c^2(t) \rangle = \frac{\dot{\gamma}^2 k_B T}{\eta_\alpha} \frac{\alpha + 1}{\Gamma(\alpha + 3)} t^{\alpha+2} + \frac{k_B T}{\eta_\alpha} \frac{t^\alpha}{\Gamma(\alpha + 1)}. \quad (5)$$

This is an interesting result, saying that flow and thermal contributions to the center-of-mass motion arise separately. Furthermore, the different qualitative behavior of the two terms, i.e., exponents of growth in time, for the two terms implies that there is a crossover taking place. To understand this in more detail, let us compare the magnitudes of the shear and thermal contributions:  $\frac{\dot{\gamma}^2 k_B T}{\eta_\alpha} \frac{\alpha+1}{\Gamma(\alpha+3)} t_c^{\alpha+2} = \frac{k_B T}{\eta_\alpha} \frac{t_c^\alpha}{\Gamma(\alpha+1)} \Rightarrow t_c^2 = \frac{\alpha+2}{\dot{\gamma}^2}$ , where  $t_c$  denotes the crossover time. As the degree of subdiffusion  $\alpha \in (0, 1)$ , the crossover time  $t_c$  is of the same order of magnitude for different  $\alpha$ . In addition, for  $t < t_c$ , the motion is subdiffusive and for  $t \geq t_c$ , the fluctuations in the center-of-mass motion grow faster than ballistic:

$$\langle x_c^2(t) \rangle \approx \frac{\dot{\gamma}^2 k_B T}{\eta_\alpha} \frac{\alpha + 1}{\Gamma(\alpha + 3)} t^{\alpha+2}. \quad (6)$$

This implies that shear contribution is dominant at large times. In other words, motion along the flow is shear dominated and thermal fluctuations play only a subdominant role. It also generalizes the earlier study on viscous shear flows ( $\alpha = 1$ ):  $\langle x_c^2(t) \rangle = \frac{2}{3} \dot{\gamma}^2 D t^3$  [25], with  $D = k_B T / 2\eta_\alpha$ . Numerical solution of Eq. (2) provides a confirmation of our analytical results (cf. Fig. 1). For shear rate unity, i.e.,  $\dot{\gamma} = 1$ , the crossover time  $\sqrt{2} \leq t_c \leq \sqrt{3}$ . This assertion is further corroborated by the numerical results in Fig. 1, where we see that motion is subdiffusive at small times, viz.  $t \lesssim 1.6$ , which is  $t_c$  for  $\alpha = 0.5$ , chosen as a representative. At longer times, the subdiffusion crosses over to a faster than ballistic motion. See Appendix C for details of the algorithm for numerical solution of Eq. (2) [26].

Interestingly, the stronger than ballistic rise of the mean-square displacement of the center of mass along shear flow

is also observed for a particle with finite mass. In other words,  $\langle x_c^2(t) \rangle \sim t^{\alpha+2}$  is robust even when we include inertia in the Eq. (2). We provide the details of this calculation in Appendix B.

### B. Relative motion for linear spring

The relative coordinate  $\mathbf{r}_r = \mathbf{r}_1 - \mathbf{r}_2$  evolves as:

$$\int_0^t dt' \eta(t-t') (\dot{\mathbf{r}}_r - \dot{\gamma} y_r \mathbf{i})(t') = -2\omega_0^2 \mathbf{r}_r + \xi_r(t), \quad (7)$$

and represents a particle moving in a harmonic potential in a viscoelastic medium under shear, with initial location at the origin. The noise variable  $\xi_r(t) = \xi_1(t) - \xi_2(t)$  is an unbiased colored Gaussian noise with correlation matrix  $\langle \xi_r(t) \xi_r^T(t') \rangle = 2k_B T \eta(|t-t'|) \mathbf{I}_3$ . As the  $y$  (and  $z$ ) component does not feel the effect of flow, its dynamics is known exactly [27,28]:

$$\begin{aligned} \langle y_r(t) y_r(t') \rangle &= 2k_B T [Q(t) + Q(t') \\ &\quad - 2\omega_0^2 Q(t)Q(t') - Q(|t-t'|)], \end{aligned} \quad (8)$$

where  $Q(t) = \frac{1}{2\omega_0^2} [1 - E_\alpha(-at^\alpha)]$  [29],  $a = \frac{2\omega_0^2}{\eta_\alpha}$ , and  $E_\alpha(\cdot)$  is the Mittag-Leffler function [30]. The motion along  $x$  direction, however, feels the effect of both thermal fluctuations and shear flow, wherein the former is known exactly, and has the form of Eq. (8):

$$\langle x_r^2(t) \rangle_{\text{Th}} = (k_B T / \omega_0^2) [1 - E_\alpha^2(-at^\alpha)]. \quad (9)$$

The shear contribution to motion in Laplace domain reads  $\tilde{x}_r(s)_{\text{Sh}} = \dot{\gamma} \tilde{G}(s) \tilde{y}_r(s)$  with  $\tilde{G}(s) = \frac{s^{\alpha-1}}{s^\alpha + a}$  and allows us to calculate the fluctuations in the relative coordinate:

$$\frac{\langle x_r^2(t) \rangle_{\text{Sh}}}{\dot{\gamma}^2} = \int_0^t dt_1 G(t-t_1) \int_0^t dt_2 G(t-t_2) \langle y_r(t_1) y_r(t_2) \rangle. \quad (10)$$

Now, using the two-point correlation of  $y$  and the following integrals:

$$\int_0^t dt_1 G(t-t_1) = t E_{\alpha,2}(-at^\alpha), \quad (11a)$$

$$\begin{aligned} \int_0^t dt_1 G(t-t_1) Q(t_1) &= (G * Q)(t) = R(t) \\ &= \frac{at^{\alpha+1}}{2\omega_0^2} E_{\alpha,2}^{(1)}(-at^\alpha), \end{aligned} \quad (11b)$$

$$\begin{aligned} \int_0^t dt_1 G(t-t_1) \int_0^t dt_2 G(t-t_2) Q(|t_1-t_2|) \\ = 2 \int_0^t dt_1 G(t_1) R(t_1), \end{aligned} \quad (11c)$$

we have:

$$\begin{aligned} \frac{\langle x_r^2(t) \rangle_{\text{Sh}}}{2\dot{\gamma}^2 k_B T} &= \frac{t^2}{\omega_0^2} \sum_0^\infty \sum_0^\infty \frac{l(-at^\alpha)^{k+l}}{\Gamma(\alpha k + 1) \Gamma(\alpha l + 2) [\alpha(k+l) + 2]} \\ &\quad + \frac{t^2}{2\omega_0^2} [2at^\alpha E_{\alpha,2}(-at^\alpha) E_{\alpha,2}^{(1)}(-at^\alpha) \\ &\quad - a^2 t^{2\alpha} \{E_{\alpha,2}^{(1)}(-at^\alpha)\}^2], \end{aligned} \quad (12)$$

where  $E_{\alpha,\beta}(\cdot)$  is the two-parameter Mittag-Leffler function and  $E_{\alpha,\beta}^{(1)}(\cdot)$  its derivative [30]. Hence, the fluctuations in the relative separation of the monomers connected by the linear spring grow with time as:

$$\langle x_r^2(t) \rangle = \langle x_r^2(t) \rangle_{\text{Th}} + \langle x_r^2(t) \rangle_{\text{Sh}}. \quad (13)$$

With  $E_\alpha(-at^\alpha)$  approaching zero as time grows, the thermal contribution to  $\langle x_r^2(t) \rangle$  eventually saturates. This, however, is not the case for the shear contribution. In order to assess the long-time behavior of  $\langle x_r^2(t) \rangle_{\text{Sh}}$ , let us make an approximation, viz.  $\frac{l}{\alpha(k+l)+2} \approx \frac{l}{2}$ , which is expected to hold for small values of  $\alpha$ , for the first term in Eq. (12). This results in:

$$\begin{aligned} \frac{t^2}{\omega_0^2} \sum_0^\infty \sum_0^\infty \frac{l(-at^\alpha)^{k+l}}{\Gamma(\alpha k + 1) \Gamma(\alpha l + 2) [\alpha(k+l) + 2]} \\ \approx \frac{t^2}{\omega_0^2} \sum_0^\infty \frac{(-at^\alpha)^k}{\Gamma(\alpha k + 1)} \sum_1^\infty \frac{l}{2} \frac{(-at^\alpha)^l}{\Gamma(\alpha l + 2)} \\ = -\frac{at^{2+\alpha}}{2\omega_0^2} E_\alpha(-at^\alpha) E_{\alpha,2}^{(1)}(-at^\alpha) \\ \sim -\frac{t^{2-2\alpha}}{2a^2\omega_0^2 \Gamma(1-\alpha) \Gamma(2-\alpha)}, \end{aligned} \quad (14)$$

where in the last step we have used the asymptotic forms of Mittag-Leffler function and its derivative, viz.  $E_{\alpha,\beta}(-at^\alpha) \sim \frac{t^{-\alpha}}{a\Gamma(\beta-\alpha)}$  and  $E_{\alpha,\beta}^{(1)}(-at^\alpha) \sim \frac{t^{-2\alpha}}{a^2\Gamma(\beta-\alpha)}$  for  $at^\alpha \gg 1$  [31]. Using the asymptotic forms in the second term in Eq. (12) and adding the long-time contribution from the first, we have:

$$\langle x_r^2(t) \rangle_{\text{Sh}} \sim \frac{\alpha \dot{\gamma}^2 k_B T}{a^2 \omega_0^2 \Gamma^2(2-\alpha)} t^{2-2\alpha}. \quad (15)$$

This implies that the shear contribution to the motion of the relative coordinate grows without bounds in a superdiffusive manner ( $\alpha$  is small). In addition, even as the thermal contribution eventually reaches a steady value, the fate of separation between the two masses is shear dominated, and  $\langle x_r^2(t) \rangle \sim t^\beta$  with  $\beta = 2(1-\alpha)$  (for small  $\alpha$ ). For arbitrary values of  $\alpha$ , such a closed form expression is not possible, and we solve Eq. (7) numerically to assess the behavior of fluctuations in the separation of the two masses. We show the results for  $\langle x_r^2(t) \rangle$  in Fig. 2(a) for different values of  $\alpha$ . For the entire range of  $\alpha \in (0, 1)$ , Fig. 2(b) shows that the fluctuations in the relative coordinate go from superdiffusive to diffusive to subdiffusive as  $\alpha$  grows from 0 to 1. The deviation from the straight line behavior is also evident, implying toward the failure of the approximation made to decouple the series in Eq. (12). The result in Fig. 2(b) also implies that the relative separation between the monomers of the Hookean spring does not achieve a steady state.

Nonexistence of the steady state for the motion of the relative coordinates implies that the system does not feel the effects of confinement. This means that the zero crossing times of the relative variable along the shear flow direction  $x_r = x_1 - x_2$  does not possess a well-defined mean. As tumbling is nothing but the zero crossing of the relative variable  $x_r$ , lack of a well-defined mean time for the Hookean spring implies that tumbling cannot be addressed within the domains

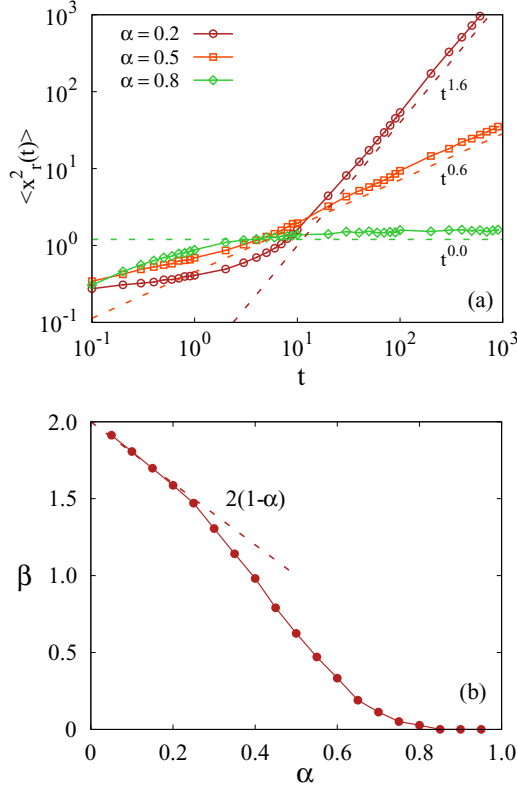


FIG. 2. (a) Mean-square displacement of the relative motion  $x_r$  along the shear flow direction for various  $\alpha$ , with respective line fits. (b) Dependence of  $\beta$  on the exponent of subdiffusion  $\alpha$ . Parameters for the numerical calculation are  $\dot{\gamma} = 1$ ,  $\eta_\alpha = 1$ ,  $2k_B T = 1$ , and  $\omega_0 = 1$ .

of linear interaction. In other words, the harmonically interacting dumbbell which serves as a starting point for addressing tumbling in viscous shear flows, e.g., Rouse chains [32,33], is not appropriate for describing tumbling motion in viscoelastic medium under shear.

For the Hookean spring, the nonexistence of steady state in shear flow is attributed to the absence of any terminal relaxation time in the memory kernel representing noise correlations. Alternatively, the noise correlation here decays as a power law at all times. In any finite-size system, however, these power-law decays are expected to be tamed beyond a certain point in time. The resulting correlation:  $\eta(t) = \eta_\alpha t^{-\alpha} e^{-t/\mathfrak{T}} / \Gamma(1 - \alpha)$ , where  $\mathfrak{T}$  is the terminal relaxation time, signifies that after time  $\mathfrak{T}$  the correlation decays exponentially. This form of noise correlation is interesting in its own right, particularly in cases where a crossover from anomalous to normal diffusion [34] is observed. However, in the present work we are interested mainly in subdiffusion, and hence we restrict ourselves to power-law decay forms of noise correlation.

Furthermore, a harmonic spring which does not put a hard cutoff on maximal allowed separation between the monomers is rather an idealization, more like a beautiful construct to derive exact results rigorously. Hence, a more realistic system which exhibits a steady state is better suited to address tumbling in subdiffusive media. We get about this by replacing the

linear spring by a nonlinear one. Inclusion of nonlinearity in the spring allows only a finite range of extension, constraining the system to relax to a steady state. This allows us to study tumbling in viscoelastic shear flows, staying within the realm of subdiffusion.

### III. GENERALIZED LANGEVIN EQUATION IN SHEAR FLOWS-NONLINEAR DUMBBELL MODEL

In order to bring in nonlinearity in the problem, we introduce FENE-LJ potential which is more realistic compared to the harmonic interaction [16]. The interparticle interaction is a contribution from both repulsive and attractive parts, viz.  $V = V_{LJ} + V_{FENE}$ , wherein

$$V_{LJ}(r) = 4\varepsilon[(\sigma/r)^{12} - (\sigma/r)^6], \quad \text{and} \quad (16a)$$

$$V_{FENE}(r) = -(kR_0^2/2) \ln[1 - (r/R_0)^2]. \quad (16b)$$

As mentioned earlier, we consider only the repulsive part of  $V_{LJ}$ . In above equations,  $r = |\mathbf{r}_1 - \mathbf{r}_2|$  denotes the separation between the two monomers,  $\sigma$  their size,  $\varepsilon$  the strength of repulsion,  $R_0$  the maximum extension, and  $k$  the stiffness constant. The force on particle  $i$  due to  $j$  is  $-\nabla_i V(|\mathbf{r}_i - \mathbf{r}_j|)$ , with  $i, j = 1, 2$ . The resulting equations of motion read:

$$\begin{aligned} \ddot{\mathbf{r}}_i + \int_0^t dt' \eta(t-t') (\dot{\mathbf{r}}_i - \dot{\gamma} y_i \mathbf{i})(t') \\ = -\nabla_i V(|\mathbf{r}_i - \mathbf{r}_j|) + \dot{\gamma} y_i \mathbf{i} + \xi_i(t), \end{aligned} \quad (17)$$

with  $i, j = 1, 2$  and  $i \neq j$ . We have retained the acceleration terms for the nonlinear system because of its numerical advantage (avoids root finding analogous to the overdamped case). The second term on the right-hand side of the above equations,  $\dot{\gamma} y_i$  is the coordinate-dependent contribution originating from the flow. This term arises due to the local streaming velocity along with the actual momentum [25,35]. It is to be noted that this flow-dependent term is absent in the overdamped limit. This is because in the overdamped limit there is no change in velocity, and hence, the acceleration term which results in  $\dot{\gamma} y_i$  for underdamped limit is absent in the overdamped limit. In addition, the motion of center of mass along the flow direction for underdamped limit, which behaves like a free particle with inertia, follows  $\langle x_c^2(t) \rangle \sim t^{\alpha+2}$  (see Appendix B). Unlike the harmonic spring, the nonlinear spring achieves a steady state due to the FENE-LJ potential which keeps the bond length in the interval  $(\sigma, R_0)$ . This is evident from the behavior of the mean-square displacement  $\langle x_r^2(t) \rangle$  of the relative separation between the two masses connected by the nonlinear spring (cf. Fig. 3). Following Refs. [35,36], we use  $\varepsilon = 1$ ,  $\sigma = 1$ ,  $R_0 = 1.5\sigma$ ,  $k = 30\varepsilon/\sigma^2$ ,  $k_B T = 1.2\varepsilon$ , and  $\eta_\alpha = 7.5$  in numerical solution of Eq. (17). We measure energy in units of  $\varepsilon$  and distance in units of  $\sigma$ .

The above results also imply that the nonlinear spring relaxes to a steady state in which the particles oscillate about a mean position. However, the approach to the steady state is nontrivial due to the slow relaxation. This is seen in Fig. 4, where we show the autocorrelation of the relative coordinate, i.e.,  $C(t) = \lim_{t' \rightarrow \infty} \frac{\langle x_r(t') x_r(t'+t) \rangle}{\langle x_r^2(t') \rangle}$  in the absence of shear flow. It is evident that  $C(t) \sim 1/t^\alpha$ , decaying as a power law with exponent  $\alpha$ , making the definition of timescale of relaxation  $\tau_0$  irrelevant. As a result, the dimensionless shear rate, also

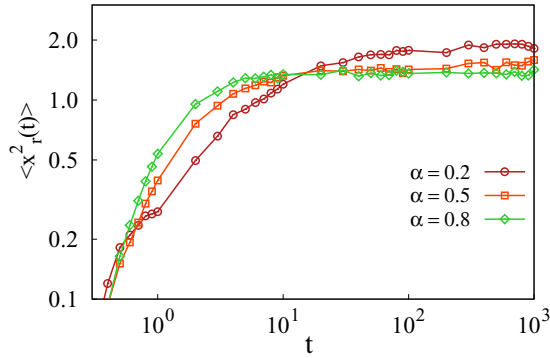


FIG. 3. Mean-square displacement of relative separation  $x_r$  of two particles connected by a nonlinear spring for different values of  $\alpha$ . The parameter values for this graph are  $\varepsilon = 1$ ,  $\sigma = 1$ ,  $R_0 = 1.5\sigma$ ,  $k = 30\varepsilon/\sigma^2$ ,  $k_B T = 1.2\varepsilon$ , and  $\eta_\alpha = 7.5$ . The shear rate  $\dot{\gamma} = 1$ .

known as the Weissenberg number, defined as  $Wi = \tau_0 \dot{\gamma}$ , cannot be assigned a value. Hence we report our findings in terms of the shear rate  $\dot{\gamma}$  only.

#### IV. DISTRIBUTION OF TUMBLING TIMES

Tumbling time  $\tau$  is defined as the interval between successive zero crossings of the relative coordinate  $x_r = x_1 - x_2$ , taking place along the flow direction. Comparing the cases of purely viscous and viscoelastic flows, at identical values of shear rate  $\dot{\gamma}$ , we find that the distribution of tumbling times  $P(\tau \geq t)$  exhibit exponentially decaying tails for either case, as observed from Figs. 5(a) and 5(b). Interestingly, however, the tumbling events taking place in viscoelastic media are slower compared to their viscous counterparts. This is not very surprising in light of the fact that the effect of viscoelasticity is to slow down the end-to-end rotation [37–39]. The exponentially decaying tails of the tumbling time distribution,  $P(\tau \geq t) \approx \exp(-\nu\tau)$ , allows us to define the characteristic tumbling time  $\tau_{\text{tumb}} = 1/\nu$ .

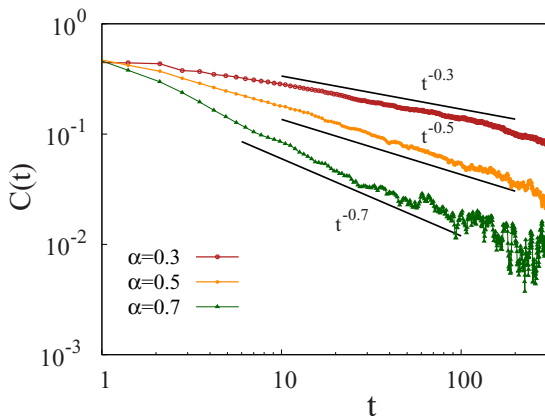


FIG. 4. Relaxation to the steady state of the nonlinear spring in the absence of flow for  $\alpha = 0.3, 0.5, 0.7$ . The black line is a fit to the curve with exponent  $\alpha$ , implying that the normalized autocorrelation  $C(t) \sim 1/t^\alpha$ . The parameters values are same as before, except that  $\dot{\gamma} = 0$ .

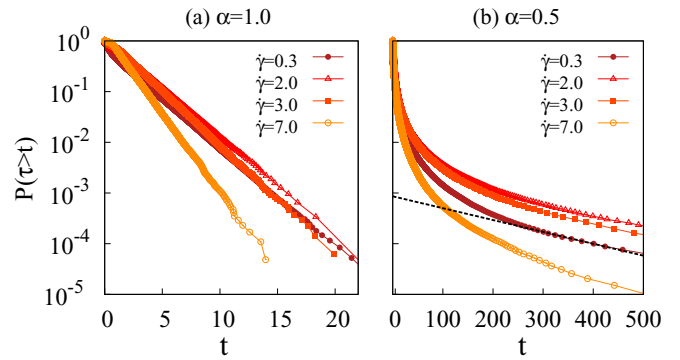


FIG. 5. Probability distribution  $P(\tau \geq t)$  for the dumbbells tumbling in (a) purely viscous shear flow ( $\alpha = 1$ ) vs (b) viscoelastic shear flows ( $\alpha = 0.5$ ). The exponentially decaying tails for the two cases are discernible from the graphs (line fit for  $\dot{\gamma} = 0.3$ ), with the distributions of the form  $P(\tau \geq t) \approx \exp(-\nu\tau)$ . In addition, a change in the trend of slope for the two types of flows is also clearly evident. The black line in (b) is a fit to demonstrate the exponentially decaying nature of the tail of the distribution.

One observation which follows immediately from Fig. 5 is that irrespective of the nature of shear flow, viz. viscous or viscoelastic, that there is a change in the trend of slope, measuring the characteristic tumbling time  $\nu$ . This is seen, if we draw a vertical line parallel to the y axis, then we find that the probability of tumbling exhibits a nonmonotonic dependence on the shear rate  $\dot{\gamma}$ . In the following subsection we shall see that this property is more pronounced for viscoelastic shear flows compared to its viscous counterpart.

#### A. Effect of subdiffusion

We study the effect of subdiffusion on tumbling of dumbbells in Fig. 6, wherein we find that the characteristic tumbling frequency  $\nu$  exhibits a nonmonotonic behavior with  $\dot{\gamma}$  which, even though present in viscous medium, is negligible compared to its viscoelastic counterparts (cf. the case of

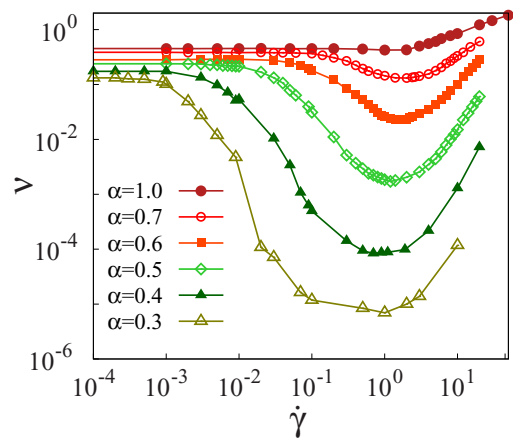


FIG. 6. Characteristic decay rate  $\nu$  vs shear rate  $\dot{\gamma}$  for subdiffusive case for different values of  $\alpha$ , including the normal diffusion case of  $\alpha = 1$  for comparison. For the subdiffusive case, the decay rate  $\nu$  achieves a minima around  $\dot{\gamma} \approx 1$ , with the depth of the minima increasing with increasing values of  $\alpha$ .

$\alpha = 1$ ). To understand this, let us first look the dependence of tumbling time on degree of subdiffusion  $\alpha$ . As we see from Eq. (17), the relative coordinate  $\mathbf{r}_1 - \mathbf{r}_2$  follows the motion of a single particle in the potential  $V = V_{\text{FENE}} + V_{\text{LJ}}$ , and in the absence of shear has its own characteristic time of zero-crossing (tumbling)  $1/\nu_0$ , where  $\nu_0$  is the tumbling frequency at zero shear rate and is dictated by the parameters of the potential and the degree of subdiffusion  $\alpha$ . As a function of the subdiffusion coefficient,  $\nu_0$  is higher for higher  $\alpha$ . This assertion is corroborated by the horizontal part of the  $\nu$  vs  $\dot{\gamma}$  graphs in Fig. 6. The reason behind this observation becomes clear once we look at the origin of subdiffusion in the viscoelastic media. As we know, it is the elastic component of the medium which results in a motion slower than diffusion. And lower is the value of  $\alpha$ , stronger is the elastic component, thereby making the negative correlations in successive displacements stronger for lower  $\alpha$ . This reflects in a longer time for zero crossing for lower  $\alpha$  system as compared to its less subdiffusive counterpart. This implies that lower  $\alpha$  results in lower  $\nu$  values. Furthermore, the trend that lower  $\alpha$  results in a lower value of  $\nu$  is also observed in the presence of shear flow, i.e.,  $\dot{\gamma} > 0$ , consistent with earlier studies on slowing down of rotation [37–39].

We observe that for very low shear rate up to  $10^{-3}$ , the tumbling frequency is unaffected by the shear flow. When  $\dot{\gamma}$  is slightly increased, we see that  $\nu$  starts to decrease with shear rate. This behavior is pronounced for the subdiffusive case ( $\alpha < 1$ ). This is because when shear rate is small but finite, it tends to keep the dumbbell aligned along the flow direction and the memory effect due to elasticity of the medium which is responsible for antipersistent motion may work as a positive feedback to the shear flow effect, thereby diminishing its tendency to rotate freely end to end. For lower  $\alpha$ , this decrease in tumbling frequency becomes more significant. This decrease in tumbling frequency, i.e., the slowing down of the tumbling motion with increasing shear rate is found to be consistent with results of previous study [37–41] due to the elasticity of the medium. Furthermore, as these studies have shown, and we also notice here, higher is the elastic component of the medium, more is the slowing down of particle motion.

An important point worth noticing, however, is that the effect of flow become evident for subdiffusive case even for smaller values of  $\dot{\gamma}$ . In other words, decrease in  $\nu$  is detectable for  $\alpha = 0.3$  for  $\dot{\gamma}$  as low as  $10^{-3}$ , while on the other hand, flow remains ineffective to  $\dot{\gamma} \approx 0.1$  for  $\alpha = 0.7$ . This is because for relative strong subdiffusion, viz. for low values like  $\alpha = 0.3$ , the slow rotating behavior can make it susceptible to the presence of even weakest of flows, whereas for relatively weaker subdiffusion, a stronger strength of flow is needed. Contrary to the behavior at low values of shear rate, for high shear rate, viz.  $\dot{\gamma}$  around 10 or so, tumbling occurs more frequently due to the increase in the rotational component of shear force dominating the tumbling dynamics. In between the two regimes, the tumbling frequency  $\nu$  hits a minima, as we observe in our numerical calculations. Interestingly, we also notice that the location of minima is  $\dot{\gamma} \approx 1$ , irrespective of the degree of subdiffusion. This is because the characteristic time of tumbling  $1/\nu_0$ , is around the same order for various values of  $\alpha$  (as seen from the horizontal part of the graphs in Fig. 6).

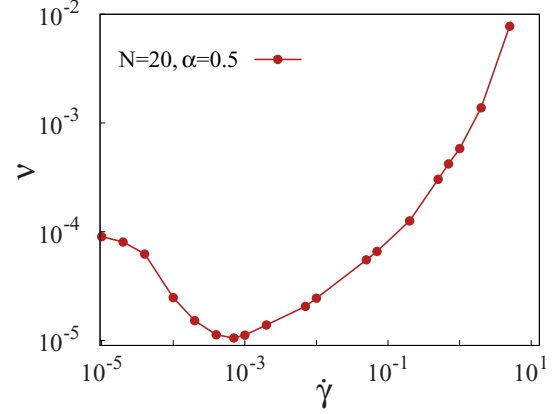


FIG. 7. Tumbling frequency  $\nu$  as a function of shear rate  $\dot{\gamma}$  for a polymer of size  $N = 20$  for the subdiffusive case  $\alpha = 0.5$ .

The graphs in Fig. 6 raise an important question regarding whether the curves of  $\nu$  vs  $\dot{\gamma}$  for different  $\alpha$  shall merge into each other at higher shear rates or exhibit different behavior. For example, it is well known that for high shear rates, the characteristic frequency  $\nu \sim \dot{\gamma}^{0.67}$  [12,13,42–46], for normally diffusing dumbbells and polymers. Will the same relation generalize to the case of subdiffusion, with an  $\alpha$ -dependent exponent  $\mu(\alpha)$ , viz.  $\nu \sim \dot{\gamma}^{\mu(\alpha)}$ ? In other words, shall there emerge different scaling behaviors in the limit of very large shear rates  $\dot{\gamma}$ , or will different degrees of subdiffusion result in different scaling each? An answer in this direction could be that when shear rates are very high, then the characteristic timescale dictated by  $\dot{\gamma}$  is the dominant one, compared to the characteristic timescale of tumbling  $1/\nu$ . And in this regime, it might be the case that tumbling frequency turns out to be a function of  $\dot{\gamma}$  only, and the  $\alpha$ -dependent contributions average out in some way. However, we are not in a position to answer based on our present study, and shall see through this in a future work.

### B. Effect of spring extension

So far we have kept the extension of the nonlinear spring fixed to  $R_0 = 1.5\sigma$ . With the size of the monomers being  $\sigma$ , this implies that extension can increase to 50% of its size. Under this condition, the spring behaves like a rigid rod. Now, changing the maximal allowed extension  $R_0$  does not significantly affect the location of the minima of the FENE-LJ potential. This corresponds to the fact that the equilibrium separation remains almost constant. Furthermore, tumbling is a property of the end-to-end rotation along the direction of shear flow. Changing the extension of the nonlinear spring does not add any direction specific properties. This implies that increasing the limit of maximal allowed extension of the spring shall not have an appreciable effect on the characteristic time of tumbling.

### C. Generalization to polymers

As a generalization to the realm of polymers, we extend our study to a small polymer of size  $N = 20$  in Fig. 7 for athermal good solvent conditions.

We find that similar to the case of dumbbells, the  $\nu$  vs  $\dot{\gamma}$  curve exhibits a nonmonotonic behavior, with the tumbling frequency  $\nu$  reaching a minimal for an intermediate value of shear rate  $\dot{\gamma}$  and then rising for higher values of shear rate. Other details like conformational changes and their statistics shall be taken up in a future work.

## V. CONCLUSION

Viscoelasticity is more of a rule rather than exception, and motivated by this, we have studied in this paper the transport and tumbling properties of polymers in a viscoelastic fluid under shear. Using dumbbells as representative, we provide analytical results for the motion of center of mass and separation between the two masses. For the simplest case of a harmonic spring connecting the two masses, we find that the mean-square displacement of the center of mass follows:  $\langle x_c^2(t) \rangle \sim \dot{\gamma}^2 t^{\alpha+2}$ ,  $0 < \alpha < 1$ , generalizing the earlier result:  $\langle x_c^2(t) \rangle \sim \dot{\gamma}^2 t^3$  ( $\alpha = 1$ ). On the other hand, fluctuations in the relative coordinate also grow monotonically with time, with  $\langle x_r^2(t) \rangle \sim t^\beta$ , where  $\beta = 2(1 - \alpha)$  to  $\alpha \approx 0.25$  and approaches 0 as  $\alpha$  approaches unity. Consequently, the system of two masses connected by a harmonic spring does not achieve a steady state. In other words, the extensively studied Rouse polymer is inappropriate to address the dynamics of polymers in viscoelastic medium under shear. We remedy this pathology by introducing a nonlinear spring in the form of FENE-LJ interaction which restricts the separation of the two masses to a maximum allowed limit. Employing the nonlinearity in the system we address tumbling of dumbbells and find that the effect of viscoelasticity in medium is to slow down the tumbling behavior. We find that the tumbling frequency  $\nu$  exhibits a nonmonotonic behavior as a function of shear rate  $\dot{\gamma}$ , with the location of minima around  $\dot{\gamma} \approx 1$ . We also find that the tumbling frequency of the dumbbells remains unaffected by the extension allowed in the nonlinear spring, making it a robust feature of the system. We hope that our work motivates further studies along this direction, particularly the effect of hydrodynamic interactions on tumbling aspects.

## ACKNOWLEDGMENTS

We thank Dibyendu Das for insightful discussions. S.S. and S.K. also acknowledge the financial assistance from SERB and INSPIRE program of DST, New Delhi, India. We also thank the anonymous reviewer for his critical and insightful comments that has helped us improve the manuscript.

## APPENDIX A: VISCOUS LIMIT OF THE POWER-LAW MEMORY KERNEL

The friction kernel for the generalized Langevin equation describing motion in the viscoelastic medium reads:  $\eta(t) = \eta_\alpha |t|^{-\alpha} / \Gamma(1 - \alpha)$ . Let there exist  $\epsilon > 0$ , then

$$\begin{aligned} \lim_{\epsilon \rightarrow 0} \lim_{\alpha \nearrow 1} \int_{-\epsilon}^{\epsilon} dt \eta(t) &= 2\eta_\alpha \lim_{\epsilon \searrow 0} \lim_{\alpha \nearrow 1} \int_0^{\epsilon} dt \frac{t^{-\alpha}}{\Gamma(1 - \alpha)} \\ &= 2\eta_\alpha \lim_{\epsilon \searrow 0} \lim_{\alpha \nearrow 1} \int_0^{\epsilon} dt \frac{1}{\Gamma(1 - \alpha)} \frac{t^{1-\alpha}}{1 - \alpha} \Big|_0^{\epsilon} \\ &= 2\eta, \end{aligned} \quad (\text{A1})$$

where we have used  $\eta_\alpha = \eta$  in the last line. As the integral of the memory kernel in a neighborhood of  $t = 0$  equates to unity, and at other times goes to zero due to divergence in the  $\Gamma$  function in the denominator, it implies that  $\lim_{\alpha \nearrow 1} \eta(t) = 2\eta\delta(t)$ .

## APPENDIX B: EFFECT OF INERTIA ON MOTION OF FREE PARTICLE IN SHEAR FLOW

The equations of motion for a particle moving in a viscoelastic medium under shear flow reads:

$$\ddot{x}_c(t) = - \int_0^t dt' \eta(t - t') (\dot{x}_c - \dot{\gamma} y_c)(t') + \dot{\gamma} \dot{y}_c(t) + \xi_{cx}(t), \quad (\text{B1a})$$

$$\ddot{y}_c(t) = - \int_0^t dt' \eta(t - t') \dot{y}_c(t') + \xi_{cy}(t), \quad (\text{B1b})$$

wherein we consider motion of only two coordinates, as the motion along  $z$  axis is identical to motion along  $y$  axis. In Laplace domain the equations transform to:

$$\tilde{x}_c(s) = \frac{\dot{\gamma} \tilde{y}_c(s)}{s} + \frac{\tilde{\xi}_{cx}(s)}{s[s + \tilde{\eta}(s)]}. \quad (\text{B2})$$

This allows us to calculate the two point position correlation of the center-of-mass motion along shear direction in Laplace domain:

$$\langle \tilde{x}_c(s) \tilde{x}_c(s') \rangle = \dot{\gamma}^2 \frac{\langle \tilde{y}_c(s) \tilde{y}_c(s') \rangle}{ss'} + \langle \tilde{\xi}_{xc}(s) \tilde{\xi}_{xc}(s') \rangle \tilde{I}(s) \tilde{I}(s'), \quad (\text{B3})$$

where  $\tilde{I}(s) = \tilde{G}(s)/s$  and  $1/\tilde{G}(s) = s + \tilde{\eta}(s)$ . Also, define  $\tilde{J}(s) = \tilde{I}(s)/s$ , in terms of which the first term of the above equation can be written as:

$$\begin{aligned} \frac{\langle \tilde{y}_c(s) \tilde{y}_c(s') \rangle}{ss' k_B T / 2} &= \tilde{J}(s) \tilde{J}(s') \frac{\tilde{\eta}(s) + \tilde{\eta}(s')}{s + s'}, \\ &= \frac{\tilde{G}(s) + \tilde{G}(s')}{s^2 s'^2 (s + s')} - \tilde{J}(s) \tilde{J}(s'), \\ &= \frac{\tilde{J}(s)}{ss'^2} - \frac{\tilde{J}(s)}{s^2 s'} + \frac{\tilde{J}(s')}{s^2 s'} - \frac{\tilde{J}(s')}{ss'^2} \\ &\quad + \frac{\tilde{J}(s)/s^2 + \tilde{J}(s')/s'^2}{s + s'} - \tilde{J}(s) \tilde{J}(s'). \end{aligned} \quad (\text{B4})$$

And the second term in Eq. (B3) reads:

$$\begin{aligned} &\langle \tilde{\xi}_{xc}(s) \tilde{\xi}_{xc}(s') \rangle \tilde{I}(s) \tilde{I}(s') \\ &= \frac{k_B T}{2} \left[ \frac{\tilde{J}(s)}{s'} + \frac{\tilde{J}(s')}{s} - \frac{\tilde{J}(s) + \tilde{J}(s')}{s + s'} - \tilde{I}(s) \tilde{I}(s') \right]. \end{aligned} \quad (\text{B5})$$

Using Eqs. (B4) and (B5) in (B3) and inverting the bivariate Laplace transform leads us to the two-time correlation of position in time domain:

$$\begin{aligned} \langle x_c(t) x_c(t') \rangle &= \frac{1}{2} \dot{\gamma}^2 k_B T [t^3 t'^3 E_{2-\alpha,4}(-\eta_\alpha t^{2-\alpha}) \\ &\quad - t^4 E_{2-\alpha,5}(-\eta_\alpha t^{2-\alpha}) + t t'^3 \\ &\quad \times E_{2-\alpha,4}(-\eta_\alpha t'^{2-\alpha}) - t'^4 E_{2-\alpha,5}(-\eta_\alpha t'^{2-\alpha}) \\ &\quad + |t - t'|^4 E_{2-\alpha,5}(-\eta_\alpha |t - t'|^{2-\alpha})] \end{aligned}$$

$$\begin{aligned}
& + \frac{1}{2}k_B T [t^2 E_{2-\alpha,3}(-\eta_\alpha t^{2-\alpha}) \\
& + t'^2 E_{2-\alpha,3}(-\eta_\alpha t'^{2-\alpha}) \\
& - |t-t'|^2 E_{2-\alpha,3}(-\eta_\alpha |t-t'|^{2-\alpha}) \\
& - tt' E_{2-\alpha,2}(-\eta_\alpha t^{2-\alpha}) E_{2-\alpha,2}(-\eta_\alpha t'^{2-\alpha})]. \quad (\text{B6})
\end{aligned}$$

From the above equation it is evident that displacement exhibits an aging behavior [47]. In addition, the presence of shear also contributes to aging separately. This is an important observation, because intuitively it is expected that the system will just run away with the shear. However, the runaway behavior is not simple, in that the system continues to age as it proceeds in time. To calculate the mean-square displacement of the center-of-mass motion along the shear, we use  $t = t'$ , which takes all the terms involving  $|t-t'|$  to zero, resulting in:

$$\begin{aligned}
\frac{\langle x_c^2(t) \rangle}{k_B T} &= \dot{\gamma}^2 t^4 [E_{2-\alpha,4}(-\eta_\alpha t^{2-\alpha}) - E_{2-\alpha,5}(-\eta_\alpha t^{2-\alpha})] \\
&+ \frac{1}{2} t^2 [2E_{2-\alpha,3}(-\eta_\alpha t^{2-\alpha}) - E_{2-\alpha,2}^2(-\eta_\alpha t^{2-\alpha})]. \quad (\text{B7})
\end{aligned}$$

Now, for  $t \gg 1$ ,  $E_{\mu,\nu} \sim t^{-\mu}/\Gamma(\nu-\mu)$  [31], which allows us to write the diffusive limit of the center-of-mass motion along the shear. Using the asymptotic form of the Mittag-Leffler function in Eq. (B7) leads us to

$$\begin{aligned}
\frac{\langle x_c^2(t) \rangle}{k_B T} &\sim \frac{\dot{\gamma}^2 t^4}{\eta_\alpha} \left[ \frac{t^{\alpha-2}}{\Gamma(\alpha+2)} - \frac{t^{\alpha-2}}{\Gamma(\alpha+3)} \right] \\
&+ \frac{t^2}{\eta_\alpha} \left[ \frac{t^{\alpha-2}}{\Gamma(\alpha+1)} - \frac{t^{2\alpha-4}}{\eta_\alpha \Gamma^2(\alpha)} \right] \\
&\sim \frac{\dot{\gamma}^2}{\eta_\alpha} \left[ \frac{t^{\alpha+2}}{\Gamma(\alpha+2)} - \frac{t^{\alpha+2}}{\Gamma(\alpha+3)} \right] \\
&+ \frac{1}{\eta_\alpha} \left[ \frac{t^\alpha}{\Gamma(\alpha+1)} - \frac{t^{2\alpha-2}}{\eta_\alpha \Gamma^2(\alpha)} \right] \\
\Rightarrow \langle x_c^2(t) \rangle &\sim \frac{\dot{\gamma}^2 k_B T}{\eta_\alpha} \frac{\alpha+1}{\Gamma(\alpha+3)} t^{\alpha+2}, \quad (\text{B8})
\end{aligned}$$

at long times. This is identical to the result for overdamped limit of motion, derived in Sec. II A.

### APPENDIX C: EMBEDDING FOR OVERDAMPED MOTION IN SHEAR FLOW

For simplicity, we discuss the concept for a single particle moving in the  $x$ - $y$  plane in a viscoelastic fluid experiencing shear along the  $x$  axis. The generalized Langevin equation describing the overdamped dynamics reads:

$$\int_0^t dt' \eta(t-t') (\dot{x} - \dot{\gamma}y)(t') = -V'_x(x, y) + \xi_x(t), \quad (\text{C1a})$$

$$\int_0^t dt' \eta(t-t') \dot{y}(t') = -V'_y(x, y) + \xi_y(t), \quad (\text{C1b})$$

where  $\xi_{x,y}(t)$  are Gaussian random variables with correlations

$$\langle \xi_x(t) \xi_y(t') \rangle = \delta_{xy} k_B T \eta(|t-t'|). \quad (\text{C2})$$

The friction kernel is a power-law decaying function of time:  $\eta(t) = \eta_\alpha t^{-\alpha}/\Gamma(1-\alpha)$  with  $0 < \alpha < 1$ . In order to solve Eq. (D1), we employ the technique of Markovian embedding. We follow the review by Goychuk [26] and outline the methodology here for motion in shear flow. As only the  $x$  coordinate involves a contribution from shear flow, we focus only on motion along the  $x$  direction. Define  $u_i = -k_i(x - \dot{\gamma} \int_0^t dt' y(t') - x_i)$ , where  $x_i$  are auxiliary variables following

$$\eta_i \dot{x}_i = k_i u_i + \sqrt{2\eta_i k_B T} \xi_i(t), \quad (\text{C3})$$

with  $k_i = C_\alpha(b) \eta_\alpha v_0^\alpha / [b^{\alpha(i-1)} \Gamma(1-\alpha)]$  and  $\eta_i = C_\alpha(b) \eta_\alpha v_0^{\alpha-1} b^{(1-\alpha)(i-1)} / \Gamma(1-\alpha)$  (cf. Eq. (23) in Ref. [26]). The numbers  $k_i$  and  $\eta_i$  define the Ornstein-Uhlenbeck processes,

$$\dot{\xi}_{i,x}(t) = -v_i \xi_{i,x}(t) + \sqrt{2k_i v_i k_B T} \xi_{i,x}(t), \quad (\text{C4})$$

and are useful in approximating the power-law decay form with a sum of exponentials as  $\eta(t) = \sum_i k_i e^{-v_i t}$ , where  $v_i = k_i/\eta_i$ . The idea of representing power-law decay with such a form is fairly old [48]. The equivalence of Eqs. (C1) and (C3) is easily shown, thus providing a way to numerically solve the former.

### APPENDIX D: MARKOVIAN EMBEDDING FOR UNDERDAMPED MOTION IN SHEAR FLOW

The generalized Langevin equation describing the dynamics of an underdamped particle in the  $x-y$  plane with a shear flow along  $x$  axis reads:

$$\ddot{x} + \int_0^t dt' \eta(t-t') (\dot{x} - \dot{\gamma}y)(t') = -V'_x(x, y) + \dot{\gamma} \dot{y} + \xi_x(t), \quad (\text{D1a})$$

$$\ddot{y} + \int_0^t dt' \eta(t-t') \dot{y}(t') = -V'_y(x, y) + \xi_y(t), \quad (\text{D1b})$$

where the symbols retain their usual meaning. The Markovian embedded form for the above equation in terms of auxiliary variables  $\{u_{i,x}\}_{i=1}^N$  and  $\{u_{i,y}\}_{i=1}^N$  is

$$\dot{x} = v_x, \quad (\text{D2a})$$

$$\dot{v}_x = -V'_x(x, y) + \dot{\gamma} \dot{y} + \sum_{i=1}^N u_{i,x}(t), \quad (\text{D2b})$$

$$\dot{u}_{i,x} = -k_i(v_x - \dot{\gamma}y) - v_i u_{i,x} + \sqrt{2v_i k_i k_B T} \xi_{i,x}(t), \quad (\text{D2c})$$

$$\dot{y} = v_y, \quad (\text{D2d})$$

$$\dot{v}_y = -V'_y(x, y) + \sum_{i=1}^N u_{i,y}(t), \quad (\text{D2e})$$

$$\dot{u}_{i,y} = -k_i v_y - v_i u_{i,y} + \sqrt{2v_i k_i k_B T} \xi_{i,y}(t), \quad (\text{D2f})$$

where  $\xi_{i,x}$  and  $\xi_{i,y}$  are Gaussian white noise variables with mean zero and with correlations:  $\langle \xi_{i,x}(t)\xi_{j,y}(t') \rangle = \delta_{ij}\delta_{xy}\delta(t-t')$ . Now, from Eq. (D2c), we have:

$$u_{i,x}(t) = -\int_0^t dt'(v_x - \dot{\gamma}y)(t')k_i e^{-v_i(t-t')} + \int_0^t dt' \sqrt{2v_i k_i k_B T} \xi_{i,x}(t') e^{-v_i(t-t')},$$

wherein we have used the initial conditions  $u_{i,x}(0) = 0$ . Substituting this in (D2b) we have

$$\dot{v}_x = -V'_x(x, y) + \dot{\gamma}y - \int_0^t dt'(v_x - \dot{\gamma}y)(t') \sum_{i=1}^N k_i e^{-v_i(t-t')} + \sum_{i=1}^N \int_0^t dt' \sqrt{2v_i k_i k_B T} \xi_{i,x}(t') e^{-v_i(t-t')},$$

$$= -V'_x(x, y) + \dot{\gamma}y - \int_0^t dt'(v_x - \dot{\gamma}y)(t')\eta(t-t') + \xi_x(t),$$

where to obtain the last step we have used the solution of Eq. (C4) and  $\xi_x(t) = \sum_i \zeta_{i,x}(t)$ . Similar calculations for the  $y$  coordinate show the equivalence of Eq. (D1) to the Markov embedded form (D2). An important difference to be noted from the case of embedded form for overdamped motion is the absence of memory term for the underdamped dynamics.

It is noted that the representation of a power-law decaying function with a sum of exponentials serves a good approximation to the former only in a finite range  $[t_i, t_f]$ , beyond which there are exponential cutoffs. For all practical purposes, like the one considered here, the range  $[t_i, t_f]$  is sufficient. Following Ref. [26], we use an  $N = 16$  term exponential approximation for the power-law decaying memory kernel employing decade scaling  $b = 10$ . Also, the fastest timescale  $v_0 = 10^3$ .

- 
- [1] J. C. Maxwell, *Philos. Trans. R. Soc. Lond.* **157**, 49 (1867).  
[2] R. S. Lakes, *Viscoelastic Solids* (CRC Press, Boca Raton, FL, 1999).  
[3] R. A. L. Jones, *Soft Condensed Matter* (Oxford University Press, Oxford, 2002).  
[4] J.-H. Jeon and R. Metzler, *Phys. Rev. E* **81**, 021103 (2010).  
[5] B. B. Mandelbrot and J. W. van Ness, *SIAM Rev.* **10**, 422 (1968).  
[6] J. Szymanski and M. Weiss, *Phys. Rev. Lett.* **103**, 038102 (2009).  
[7] S. C. Weber, A. J. Spakowitz, and J. A. Theriot, *Phys. Rev. Lett.* **104**, 238102 (2010).  
[8] I. Bronstein, Y. Israel, E. Kepten, S. Mai, Y. Shav-Tal, E. Barkai, and Y. Garini, *Phys. Rev. Lett.* **103**, 018102 (2009).  
[9] D. E. Smith, H. P. Babcock, and S. Chu, *Science* **283**, 1724 (1999), and references therein.  
[10] P. LeDuc, C. Haber, G. Bao, and D. Wirtz, *Nature* **399**, 564 (1999).  
[11] F. B. Usabiaga and R. Delgado-Buscalioni, *Macromol. Theory Simul.* **20**, 466 (2011).  
[12] C. M. Schroeder, R. E. Teixeira, E. S. G. Shaqfeh, and S. Chu, *Phys. Rev. Lett.* **95**, 018301 (2005).  
[13] R. G. Winkler, *Phys. Rev. Lett.* **97**, 128301 (2006).  
[14] N. Özkaya and M. Nordin, *Fundamentals of Biomechanics* (Springer, New York, 1999), pp. 195–218.  
[15] M. Herrchen and H. C. Öttinger, *J. Non-Newtonian Fluid Mech.* **68**, 17 (1997).  
[16] K. Kremer and G. S. Grest, *J. Chem. Phys.* **92**, 5057 (1990).  
[17] R. Zwanzig, *J. Stat. Phys.* **9**, 215 (1973).  
[18] R. Kubo, *Rep. Prog. Phys.* **29**, 255 (1966).  
[19] P. E. Rouse, *J. Chem. Phys.* **21**, 1272 (1953).  
[20] U. Weiss, *Quantum Dissipative Systems*, 2nd ed. (World Scientific, Singapore, 1999).  
[21] R. Kupferman, *J. Stat. Phys.* **114**, 291 (2004).  
[22] A. Gemant, *Phys.* **7**, 311 (1936).  
[23] I. Goychuk, *Phys. Rev. E* **80**, 046125 (2009).  
[24] K. G. Wang and M. Tokuyama, *Physica A* **265**, 341 (1999).  
[25] M. G. McPhie, P. J. DAVIS, I. K. Snook, J. Ennis, and D. J. Evans, *Physica A* **299**, 412 (2001).  
[26] I. Goychuk, *Adv. Chem. Phys.* **150**, 187 (2012).  
[27] A. D. Viñales and M. A. Despósito, *Phys. Rev. E* **73**, 016111 (2006).  
[28] M. A. Despósito and A. D. Viñales, *Phys. Rev. E* **77**, 031123 (2008).  
[29] M. A. Despósito and A. D. Viñales, *Phys. Rev. E* **80**, 021111 (2009).  
[30] I. Podlubny, *Fractional Differential Equations* (Academic Press, San Diego, CA, 1999).  
[31] J. R. Wang, Y. Zhou, and D. O'Regan, *Integr. Transf. Spec. Funct.* **29**, 91 (2018).  
[32] S. Bhattacharya, D. Das, and S. N. Majumdar, *Phys. Rev. E* **75**, 061122 (2007).  
[33] D. Das and S. Sabhapandit, *Phys. Rev. Lett.* **101**, 188301 (2008).  
[34] D. Molina-Garcia, T. Sandev, H. Safdari, G. Pagnini, A. Chechkin, and R. Metzler, *New J. Phys.* **20**, 103027 (2018).  
[35] S. Singh and S. Kumar, *J. Chem. Phys.* **150**, 024906 (2019).  
[36] G. S. Grest and K. Kremer, *Phys. Rev. A* **33**, 3628 (1986).  
[37] G. D'Avino, N. A. Hulsen, K. Snijkers, N. Vermant, O. Greco, and P. L. Maffettone, *J. Rheol.* **52**, 1331 (2008).  
[38] F. Snijkers, G. D'Avino, R. A. Maffettone, O. Greco, M. Hulsen, and J. Vermant, *J. Rheol.* **53**, 459 (2009).  
[39] K. D. Housiadas and R. I. Tanner, *Phys. Fluids* **30**, 073101 (2018).  
[40] M. Astruc, S. Vervoort, H. O. Nouatin, T. Coupeuz, Y. De Puydt, P. Navard, and E. Peuvrel-Disdier, *Rheol. Acta* **42**, 421 (2003).  
[41] W. R. Hwang and M. A. Hulsen and H. E. H. Meijer, *J. Non-Newton. Fluid Mech.* **121**, 15 (2004).

- [42] R. E. Teixeira, H. P. Babcock, E. S. G. Shaqfeh, and S. Chu, *Macromolecules* **38**, 581 (2005).
- [43] S. Gerashchenko and V. Steinberg, *Phys. Rev. Lett.* **96**, 038304 (2006).
- [44] A. Celani, A. Puliafito, and K. Turitsyn, *Europhys. Lett.* **70**, 464 (2005).
- [45] A. Puliafito and K. Turitsyn, *Physica D* **211**, 9 (2005).
- [46] H. Kobayashi and R. Yamamoto, *Phys. Rev. E* **81**, 041807 (2010).
- [47] N. Pottier, *Physica A* **317**, 371 (2003).
- [48] R. G. Palmer, D. L. Stein, E. Abrahams, and P. W. Anderson, *Phys. Rev. Lett.* **53**, 958 (1984).

*Correction:* Minor typographical errors were found in Eq. (2) and in the inline equation appearing in the second complete sentence after Eq. (2) and have been fixed. The third sentence before Sec. II B contained a text usage error and has been set right. A subscript to  $\nu$  was missing in the expression “time of tumbling  $1/\nu$ ” in the penultimate paragraph of Sec. IV A and has been inserted.